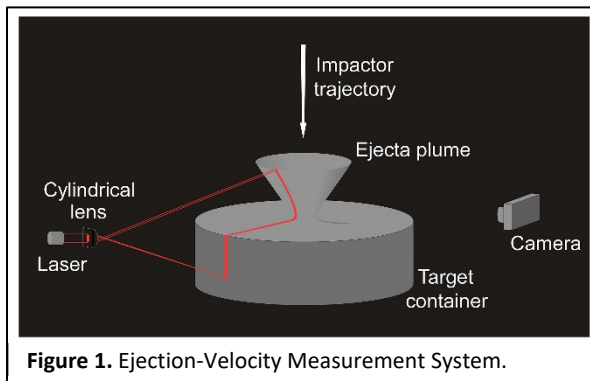


**Impacts into a Strength-Layered Target: The Time Evolution of the Excavation-Stage Flow.** J.L.B. Anderson<sup>1</sup>, M.J. Cintala<sup>2</sup>, C.J. Cline II<sup>3</sup>, L.E. Dechant<sup>1</sup>, R.A. Taitano<sup>1</sup>, and J.B. Plescia<sup>4</sup>. <sup>1</sup>Geoscience, Winona State Univ., Winona, MN 55987. <sup>2</sup>Code X13, NASA Johnson Space Center, Houston, TX 77058. <sup>3</sup>Jacobs, NASA Johnson Space Center, Houston, TX 77058. <sup>4</sup>Applied Physics Lab, Johns Hopkins Univ., Laurel, MD 20723. (Contact: JLAnderson@winona.edu)

**Introduction:** Impact cratering has dominated the evolution and modification of planetary surfaces throughout the history of the solar system. Impact craters can serve as probes to understanding the details of a planetary subsurface; for example, Oberbeck and Quaide [1,2] suggested that crater morphology can be used to estimate the thickness of a regolith layer on top of a more competent unit. Lunar craters show a morphological progression from a simple bowl shape to flat-floored and concentric craters as diameter increases for a given regolith thickness.

The final shape of the impact crater is a result of the subsurface flow-field initiated as the projectile transfers its energy and momentum to the target surface at the moment of impact. Therefore, when a regolith layer is present over a stronger substrate, such as is the case on the lunar mare, the substrate modifies the flow-field resulting in the distinctive final crater morphology. Here we report on a series of experimental impacts into targets composed of a thin (2 cm) layer of loose sand on top of a stronger substrate. We use the Ejection-Velocity Measurement System (EVMS, Fig.1) developed by [3] to examine the ejecta kinematics at specific times during the formation of these craters in strength-layered targets.



**Figure 1.** Ejection-Velocity Measurement System.

**Experiment Design:** Experimental impacts were performed in near-vacuum (< 1 torr) with 4.76-mm aluminum projectiles impacting the target at  $1.54 \text{ km s}^{-1}$  ( $\pm 0.02 \text{ km s}^{-1}$ ) and at normal incidence to the target surface. A well-sorted quartz sand (0.4-0.8 mm grain size) served as a 2-cm "regolith" layer over a stronger substrate made of chemically bonded sand (grain size < 0.5 mm). These experiments were compared to a control experiment that used a 12-cm deep target of the unbonded 0.4-0.8 mm sand [4].

The EVMS projects a vertical laser sheet perpendicular to the target surface and passing through the impact point, thus illuminating a vertical slice of the advancing ejecta curtain (Fig. 1). The laser is strobed at a pre-defined rate and particles are illuminated multiple times along their ballistic trajectories as imaged by the camera (Fig. 2). The resulting image is digitized and processed to determine ejection position, angle, and speed that are then related through scaling relationships [e.g., 3]. 3D scans were also recorded before and after each experiment, permitting close examination of the final crater morphometry with respect to the original stratigraphy of the target [5].

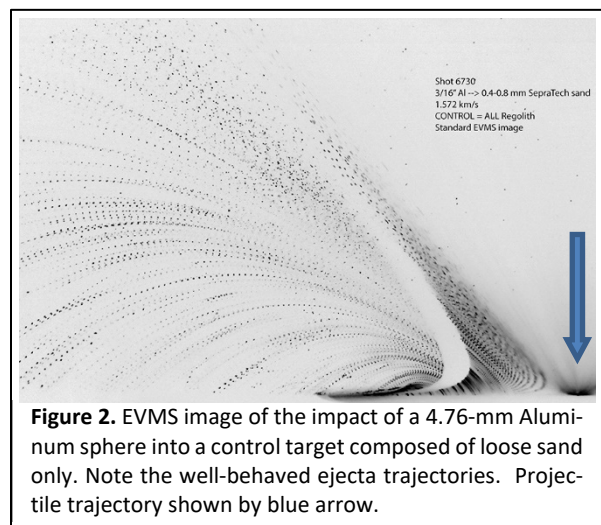


**Figure 2.** EVMS image of the impact of a 4.76-mm Aluminum sphere into a control target composed of loose sand only. Note the well-behaved ejecta trajectories. Projectile trajectory shown by blue arrow.

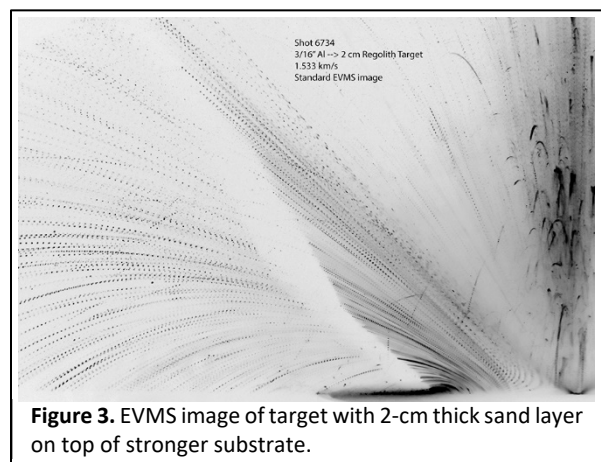


**Figure 3.** EVMS image of target with 2-cm thick sand layer on top of stronger substrate.

**Ejecta Kinematics for Impacts into Strength-Layered Targets:** As expected, the ejecta kinematics of the control target with no stronger substrate at depth was

typical for this type of experiment (Fig. 2). The addition of the stronger substrate below a 2-cm thick regolith layer, however, produced a more complex ejecta pattern including a “dogleg” or kink in the shape of the advancing ejecta curtain (Fig. 3). Notice that there are two clear ejecta components within this image: (1) the **curtain ejecta** which appear as a typical ejecta curtain moving outward with time as the crater grows and (2) the **central ejecta** that move along high-angle trajectories near to and above the impact point. These central ejecta had never before been observed in our EVMS images until a stronger substrate was added beneath an unconsolidated layer. It is clear that this portion of the excavation-stage flow is a direct result of the stronger substrate.

In order to interpret this complex excavation flow, we completed a second series of impact experiments using targets that all had a 2-cm thick layer of regolith atop the stronger substrate. Rather than strobing the EVMS laser for the entire duration of crater growth (about 600 msec), however, we set the EVMS to image the ejecta in 10-20 msec “snapshots” and captured the time-evolution of this complex excavation-stage flow and ejecta pattern (Fig. 4, A&B). In these ten experiments, the average impact speed was  $1.54 \pm 0.02$  km s<sup>-1</sup> and the average crater diameter was  $14.07 \pm 0.26$  cm, showing excellent reproducibility.

**Time-Evolution of Excavation-Stage Flow:** As expected, ejection speeds and angles within the ejecta

curtain for the strength-layered experiments decrease as the crater grows in time (Fig. 4, C&D) and are similar to those of the all-regolith control experiment.

As inferred from the EVMS image for the 2-cm regolith target (Fig. 3), the central ejecta are predominantly high angle and low speed when compared to the curtain ejecta (Fig. 4, E&F). For clarity, only three of the ten time-steps are shown in Fig. 4, but it is possible to see a general time-dependence to the ejection speeds and angles; this will be investigated in more detail as we move forward. Of particular interest is the broad range of ejection positions observed at later times for these central ejecta. We are currently looking at our curve-fitting techniques as well as possible spallation or other interactions between ejecta particles in this region of the excavation-stage flow as possible sources of these data. Should these observations hold up and scale with crater size, these results imply that self-secondary cratering [6] would require the presence of a strong subsurface layer below the impact site.

**References:** [1] Oberbeck & Quaide 1967, JGR **72**, 4697-4704. [2] Quaide & Oberbeck 1968, JGR **73**, 5247-5270. [3] Cintala *et al.* 1999, MAPS **34**. [4] Cline *et al.* 2019, AGU #3504. [5] Anderson *et al.* 2020, LPSC. [6] Plescia & Robinson 2019, Icarus **321**, 974-993.

**Acknowledgements:** This work would not have been possible without EIL gunners Frank Cardenas and Roland Montes and “Captain Electron,” Terry Byers. This work is supported by NASA SSW grant NNX16AR92G.

